PROBARTIONARY REVIEW RESEARCH REPORT

Development of advanced tracking methods for the quantification and modelling of Cardiac Progenitor Cell migration patterns in *Gallus Gallus*

Connor Reynolds

Student Number: 100127017

Primary supervisor: Simon Moxon

Second supervisor: Andrea Munsterberg

Other supervisors: Leighton Folkes and Timothy Grocott

Internal assessor: Grant Wheeler

Contents

Abstract

Cardiac cells originate from a population of progenitors which establish the early heart tube following a long-range migration event that initiates during gastrulation. After exiting the mid-anterior primitive streak, the trajectories of cardiac progenitor cells (CPCs) up to the fusion of the primitive heart tube have been previously characterised, but the role of signalling molecules on their migration and the subsequent outcome on heart development is still poorly understood. Popular and versatile software such as TrackMate have been used to track fluorescently labelled CPCs in chick embryos across time-lapsed-microscopy images, but the flexibility of these tools can come at the cost of reduced optimisation for these specific images and biological context. Here, we present a cell detection method specifically designed for capturing GFP-labelled CPCs in time-lapsed images of whole chick embryos. By using a custom Laplacian filter with a Watershed transformation, we were able to detect a population of cells closer to the ground-truth value than using TrackMate.

Chapter 1. Literature review

1.1 Introduction

The development of the heart as the first functional organ is shared amongst all amniote embryos and is initially formed during early embryogenesis as a linear structure called the heart tube, which progressively develops into a more mature heart through remodelling of the tube (Voronov et al, 2004). The cardiomyocytes that form the heart tube originate from the mesoderm-fated cardiac progenitor cells (CPCs) which, during gastrulation, ingress through the primitive streak before migrating bilaterally towards the medial-anterior of the embryo, where they contribute exclusively to the splanchnic layer of the lateral plate mesoderm as bilateral heart fields (Schoenwolf and Garcia-Martinez, 1995). During neurulation, a cardiogenic crescent establishes, where both heart fields migrate medially towards one another while the CPCs differentiate into endocardial tubes, which subsequently fuse to form a single heart tube (Stalsberg and DeHaan, 1969; Colas et al, 2000).

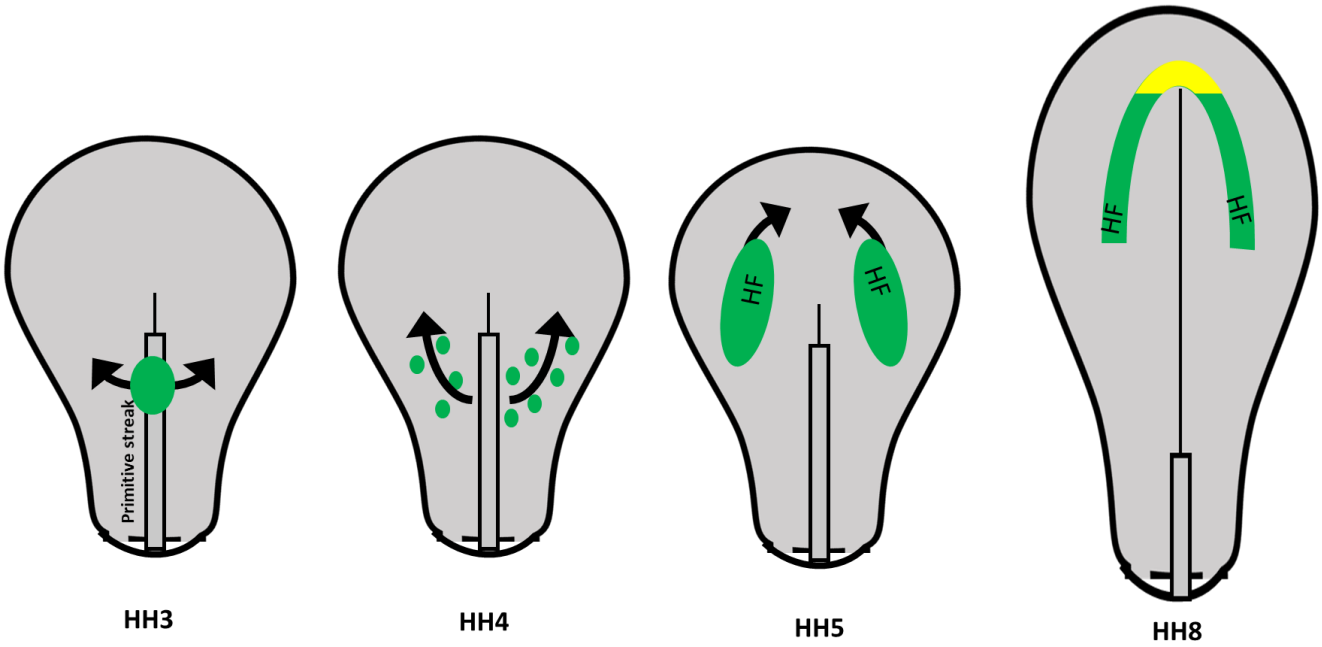

Figure 1. Migration of CPCs (green) at different referenced to Hamburg-Hamilton (HH) (1951) stages. At HH3 CPCs emerge from the mid-anterior primitive streak and migrate bilaterally towards the medial-anterior of the embryo. At HH4 the CPCs cease emerging from the primitive streak. At HH5, the cells establish bilateral heart fields specifically in the splanchnic layer of the lateral plate mesoderm, which to move medially. At HH8 the heart fields form a cardiac crescent, though it is disputed as to whether this is a single crescent or if it is separated (yellow).

The regulated early development of the heart is a critical step in embryogenesis, as congenital defects in heart tube formation can lead to cardiac dysfunction and often prenatal death of the organism such as cardia bifida, where the heart tube fails to fuse. As CPCs are the main contributors to the heart tube, it is essential that their behaviour is tightly controlled throughout early embryogenesis by morphogens or other signalling molecules. Numerous studies have shown the upregulation or knockout of different signals can result in defective heart tube fusion, with some demonstrating this is paired with abnormal CPC trajectories (Yue et al, 2008; Song et al, 2014). As the complex network of converging signals that regulate CPC movement is poorly understood, it is essential that computational techniques used to analyse and quantify their migratory behaviours across different signal treatments are regularly benchmarked and improved when necessary.

1.1.1 The chick as a model organism for cardiac development

Chicken (*Gallus gallus*) embryos are a popular experimental model organism for investigations in developmental biology, with their use predating modern molecular techniques. Early observations in developing chick embryos identified the heart as the first functional organ, defined embryos into their respective germ layers – the endoderm, mesoderm and ectoderm, and were used to support the prevailing theory that organisms develop progressively from a simpler embryonic state as opposed to being small preformed adults (reviewed by Stern, 2005). Their continued use since the onset of modern experimental embryology has led to numerous landmark discoveries in amniote development including the characterisation of migratory patterns of epiblast derived cells in gastrulation (Gräper, 1929; Wetzel, 1929), the induction of the primitive streak by the hypoblast and the identification of the Hensen's node as the organizer region in amniotes (Waddington, 1933).

Chick embryos are an attractive model for studying early cardiac development for numerous reasons, firstly being they develop *in ovo*, which makes them more accessible to manipulations compared to organisms that develop *in utero*. This means early chick embryos can be readily separated from the egg and allowed to develop in culture (Chapman et al, 2001), making them even more exposed to interventions as well as allowing for their analysis through the use of microscopy (Dormann and Weijer, 2006; Yue et al, 2008; Song et al, 2014). Additionally, like other nonrodent amniotes, the embryonic precursor cells of the chick blastocyst form as a flat and disk-shaped epiblast that allows for investigations to clearly observe cell movement and fate during gastrulation (Chuai et al, 2012).

The entire development of a normal chick embryo from egg laying to hatching was categorised into a series of 46 stages by *Hamburger and Hamilton* in 1951, and more recently a review by *Martinsen* (2005) mapped developmental landmarks in heart formation to each Hamburger-Hamilton (HH) stage, which is beneficial for researchers to use as a reference. The early stages of cardiac development are also highly conserved between chicks and humans, both of which mature into a four-chambered heart (Gittenberger-de Groot et al, 2005), meaning insights derived from the former can be highly applicable to understanding heart development and defects in humans.

1.1.2 Regulation of CPC migration and fate

The fate of avian CPCs is established pre-gastrulation, as cardiogenic precursors have been mapped to the epiblast prior to primitive streak induction (Hatada and Stern, 1994), where they are specified by activin-like signals from the hypoblast and become mostly committed to a cardiogenic fate by HH3 (Yatskievych et al, 1997). Like other mesodermal cells, the migration of CPCs away from the mid-anterior primitive streak at HH4 is regulated by a chemo-attraction and -repulsion to FGF4 expressed at the anterior and FGF8 at the posterior respectively (Yang et al, 2002). This chemotaxis towards the lateral plate mesoderm is supported by Wnt3a expression at the primitive streak and Wnt8c across the posterior region of the embryo, which both inhibit further specification of CPCs (Marvin et al, 2001), with Wnt3a also guiding their movement through chemo-repulsion (Yue et al, 2008).

Following the establishment of the heart fields at HH5, the formation of the epicardial tubes and their subsequent fusion at HH10 requires the promotion of CPC differentiation by signals at the anterior endoderm, including the Wnt inhibitor crescent (Marvin et al, 2001) and the bone morphogenetic proteins (BMP) BMP2 and BMP4, which are known to induce the cardiogenic transcription factor Nkx2.5 (Schultheiss et al, 1997). The dysregulation of these signals can disrupt cardiogenesis, with overexpression of Wnt3a near the lateral plate mesoderm or BMP2/4 near the mid-primitive streak leading to significantly wider CPC migration trajectories that results in cardia bifida (Yue et al, 2008; Song et al, 2014). Additionally, if BMP2/4 signals are not inhibited by chordin at the mid-anterior primitive streak prior to gastrulation, cardiogenesis does not occur (Ladd et al, 1998).

Other signals such as the activin antagonist follistatin can inhibit the specification of CPCs prior to gastrulation (Yatskievych et al, 1997), but it is not known what effect it has during their migration after HH3. Overexpression of retinoic acid also interferes with the establishment of the cardiogenic crescent and can result in cardia bifida, possibly due to the fact it activates non-canonical Wnt pathways such as Wnt3a (Osmand et al, 1991; Osei-Sarfo and Gudas, 2014).

Understanding how different signal pathways control CPC migration using gain- or loss-of-function interventions in chick embryos could offer important insights in the causes of cardia bifida or non-fatal congenital heart defects in humans. Additionally, as they are candidates for cardiac cell therapies, knowledge of regulating CPC behaviours may help in the development of new techniques to treat heart failure (Le and Chong, 2016).

1.1.3 Analysis of CPC migration

Localising CPCs is critical when studying their migration, as in standard brightfield microscopy images they are indistinguishable from the rest of the developing chick embryo. Labelling of the cardiogenic mesoderm with iron oxide was used in early investigations to show the establishment of the bilateral heart fields and their coinciding fusion with heart tube formation (deHaan, 1963), following which radiolabelling was used to develop a refined cardiogenic fate map from HH5 to the fusion of the heart tube at HH10 (Stalsberg and DeHann, 1969). Later studies using antibody labelling of grafted chick-quail chimeric cells showed CPCs leave the mid-anterior primitive streak at HH3 (Schoenwolf and Garcia-Martinez, 1995), where they migrate bilaterally towards the lateral plate mesoderm, which has more recently been demonstrated in real-time from fluorescent labelling of CPCs at the mid-anterior primitive streak with fluorescent proteins (Yue et al, 2008; Song et al, 2014).

Time-lapsed-microscopy (TLM) involves taking a series of images at specific time-points, which can be generated using microscopy techniques such as fluorescent microscopy imaging (FMI), where light of only specific wavelengths are detected (Hamilton, 2009), phase contrast (PC) imaging and differential interference contrast (DIC) imaging, both of which use the interference of light travelling through objects to generate images (Obara et al, 2013). TLM-imaging of whole chick embryos has been used since the general "polonaise" movement of cells during gastrulation was first characterised (Gräper, 1929; Wetzel, 1929), which continued throughout the development of the aforementioned cardiogenic fate maps with early isotopic labelling (Stalsberg and DeHann, 1969), but these maps were only able to investigate the fate and movement of CPCs after they have established in the splanchnic layer of the lateral plate mesoderm at HH5.

Recent advancements in cell localisation have allowed for specific embryonic cell lineages to be labelled during gastrulation using electroporation to transfect GFP expression plasmids into HH3 primitive streak cells of a donor chick embryo, after which the GFP-labelled cells are transplanted into different primitive streak regions of a host embryo, where their movement and fate can be observed (Yang et al, 2002). Through this method, it is now possible to generate fluorescent TLM-images that can analyse GFP-labelled CPC trajectories across their entire migration from their departure of the primitive streak at HH3 to the fusion of the heart tube at HH10, which was used previously to determine the effects of Wnt3a and BMP2/4 expression in CPC movement (Yue et al, 2008; Song et al, 2014). Recent techniques have been developed to fluorescently label primitive streak cells by transfecting expression plasmids directly to study somitogenesis (Fan et al, 2018), avoiding the need for invasive cell transplantations.

Tracking CPCs is often performed using advanced techniques across the TLM-movie, where each greyscale image is represented as a matrix containing intensity values from 0-255. While it is necessary for an image matrix to contain at least two spatial dimensions (2D) matrices can be arrayed to produce images with further dimensions. Many investigations have quantified morphological features of developing embryos with the addition of another spatial plane in three dimensions (3D), but 3D imaging may also refer to an array of matrices taken across different time points, as in TLM-movies, and time-lapsed arrays of spatially 3D images are often considered four-dimensional (4D) (McColl et al, 2018). To avoid confusion in this terminology, the dimensionality of a single or time-lapsed-series of images will be referred to according to only their spatial dimensions, in which our TLM-images is 2D.

1.2 Cell Tracking overview

Tracking objects of interest (OOIs) across a time-lapsed image-series involves their detection and linkage between image frames, which are usually independent algorithms performed sequentially. For cell tracking, the approaches used by these algorithms can vary significantly depending on the resolution of the images, the microscopy techniques used and the environment of the cells during the imaging.

The first step of a cell tracking method is to detect the cells by distinguishing them as OOIs, referred to as the foreground, from regions of no interest – the background. In TLM-movies, this is performed for each image frame and, if successful, allows spatial features of each cell to be extracted for the linkage step. This step can be particularly challenging when the lighting in images is uneven or if they are saturated in noise, as this can lead to regions of the background being falsely detected as cells.

Linking cells across image-frames automatically can be computationally costly, algorithmically non-trivial and errors are rarely able to be avoided entirely, meaning that in TLM-movies with a small number of cells across a few frames, manual tracking is often preferred (Zhang and Roadway, 2007; Pinto-Teixeira et al, 2013; Myers and Krieg, 2013). In an image-series with hundreds of cells across hundreds of frames however, manual tracking would be time consuming to the point a method that is at least partially automated is required. Algorithms designed for automatic cell linkage are generally placed into two categories: model evolution, where the boundaries of detected cells are defined then linked to cells in other frames based on their degree of overlap, and detection association, as shown in figure 2, where cells are linked to others across the image-series based on their relatedness. The more common latter almost universally involves distal proximity of cells, but they can include closeness of other features such as size or shape.

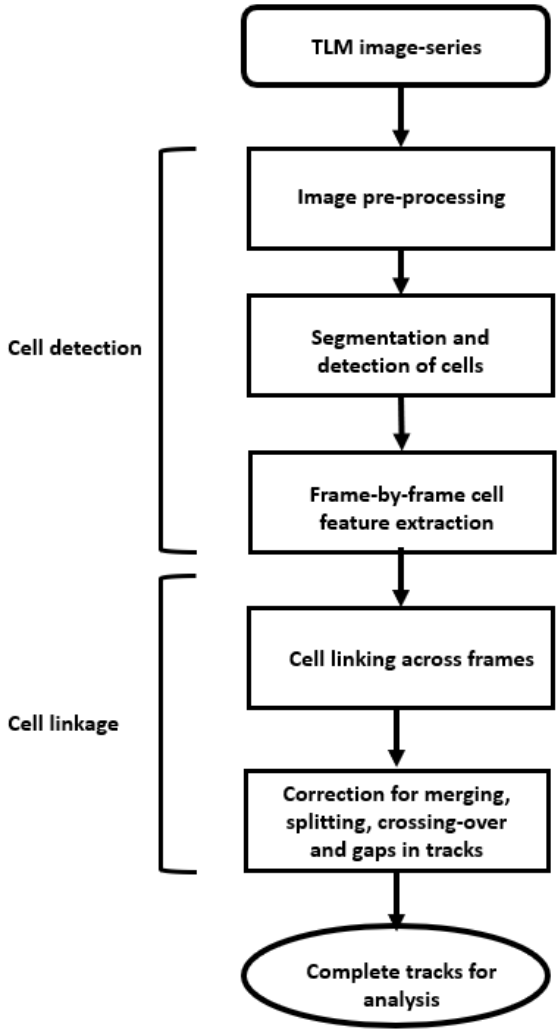

Figure 2. General approach for detection association-based cell tracking methods, involving algorithms for detecting cells in each frame following by cell-linkage. Adapted from *Hamilton, 2009.*

The increased use of TLM techniques in biomolecular research to quantify cellular, subcellular or extracellular movement patterns means there is a growing demand for improved tracking algorithms which has led to a series of competitions by the IEEE International Symposium on Biomedical Imaging – the Cell Tracking Challenges (CTCs) and Particle Tracking Challenges (PTCs), where participating researchers attempted to develop high-performing tracking pipelines for cells or particle-like signals in TLM-movies produced using different microscopy techniques across several biological contexts. The most competitive tracking pipelines produced for the CTCs and PTCs have been reviewed by *Ulman et al.* (2017) and *Chenouard et al.* (2014) respectively, both of whom showed no specific approaches were versatile enough to perform optimally across all types of images and biological processes.

It is important to note that algorithms referred nominally by the challenges as "cell trackers" are often considered distinct from "particle trackers", which are designed for tracking intracellular particle-like signals and do not consider mitotic events. In some TLM-movies of fluorescently labelled cells however, the approaches used by "particle trackers" may be superior for cell detection and linkage than nominal "cell trackers", as poorly resolved cells can appear particle-like as opposed to highly resolved cells, which often have clearly visible spatial features and intracellular structures that can be used in the linkage step.

CTC algorithms based on detection association had similar frameworks with those in the PTC, with many of the approaches used for detection and linkage being identical, the major deviance of which being most cell trackers detected division while particle trackers did not. The similarities between "cell" and "particle trackers" are further demonstrated by the fact TrackMate, a popular and widely used tracking tool that is often considered a "particle tracker" (Tinevez et al, 2017), can optionally detect division events and has been used for both single-cell (McColl et al, 2018) and intracellular molecule tracking (Tanebaum et al, 2014). For this reason, we shall consider any method which can be used for cell detection and linkage as a cell tracker.

While there is an abundance of cell tracking algorithms, most are available only as low-level libraries or source code and using them to their full potential could require extensive computational experience which many researchers do not possess. As the development of evermore competitively performing algorithms has grown, so has the demand for them to be built into software tools designed so researchers with little-to-no programming or mathematical experience can use them. A commentary by *Carpenter et al.* (2012) set several criteria for bioimaging software usability, recommending they should aim to be user-friendly, publicly available as a functional, tested and benchmarked software, modular for specific purposes, interoperable with other imaging or analysis software and have an accessible open-source code that is written idiomatically.

1.2.1 Existing software

The availability of a cell tracking software is possibly the most important of the *Carpenter et al.* criteria, as limiting the access to a tool means it is less likely to be used, documented and benchmarked compared to other more accessible tools. As shown in Table 1, many cell trackers, such as ImarisTrack (Oxford Instruments) and Volocity (Quorum Technologies) are restricted behind a paywall, the expensive access of which may discourage their use by researchers. Many freely distributed tracking software used in previous studies also fail this criterion, with tools such as CellTrack (Sacan et al, 2008), CellCognition (Held et al, 2010), DcellIQ (Li et al, 2010), TimeLapseAnalyser (Huth et el, 2011) and TLM-tracker (Klein et al, 2012) being either unsupported for modern operating systems or inaccessible for public use. Another failed criterion in all paid and some free tracking tools is the lack of open-source code for the software, which may be advantageous for researchers to review or improve the performance and power of the tracking algorithm. Some software are fully available, but appear to not function as intended, such as NucliTrack (Cooper, 2017).

Notable cell tracking tools that meet much of the usability criteria by being freely available, modular, open source, interoperable and functional in modern operating systems include the TrackMate (Tinevez et al, 2017) plugin for the software ImageJ/Fiji, CellProfiler with the TrackObjects module (McQuin et al, 2018) and Spot Tracker, a plugin for the software Icy (de Chaumont et al, 2012). These tools can be considered semi-automated as they require user input for optimal cell detection and tracking, which in high-throughput or batch processing could be problematic as TLM-image stacks can vary in quality and thus require different inputs for optimisation.

Table 1. Accessibility and functionality of different software tools for cell tracking. Green indicates potential usability, red indicates non-usability

Software	Accessibility				Supported OS		Functionality	
	Free	Publicly available	Open source	Installs compiler-free	Windows 10	Ubuntu 18.04	Runs without crashing	Language
Fiji (ImageJ) + Trackmate	✓	✓	✓	✓	✓	✓	✓	Java
CellProfiler	✓	✓	✓	✓	✓	✗	✓	Python
Icy - Spot Tracker	✓	✓	✓	✓	✓	✓	✓	Java
Nuclitrack	✓	✓	✓	✓	✓	✗	✗	Python
CellCognition	✓	✓	✓	✓	✗	✗	?	Python
DcellIQ	✓	✓	✓	✓	✗	✗	?	MATLAB
CellTrack	✓	✓	✓	✓	✗	✗	?	C+
TimeLapseAnalyzer	✓	✓	✓	✓	✗	✗	?	MATLAB
CellTracker	✓	✓	✓	✗	✓	✗	?	MATLAB
LEVER	✓	✓	✓	✗	✓	✗	?	MATLAB
TLM-tracker	✓	✗	✗	✗	✗	✗	?	MATLAB
ImarisTrack	✗	✓	✗	?	✓	✗	?	?
Volocity	✗	✓	✗	?	✓	✓	?	?

TrackMate is a tracking tool that uses particle tracking-based principles within its algorithm, but it has the option for lineage tracing and has been used previously to track singe-cells (Tinevez et al, 2017; McColl et al, 2018). Having over 500 citations across various studies, TrackMate's overall method is considered versatile and robust, using a blob detection approach followed by a frame-to-frame particle-linking algorithm called the linear assignment problem (LAP) solution, which is based on a mathematical formulation by *Jaqaman et al.* (2008). Being a plugin for ImageJ/Fiji, there are numerous pre- and post-processing tools that can be used to complement or correct the cell tracking and, as Bioformats is integrated into ImageJ, TrackMate can also analyse imaging data of many file types without formatting issues, including videos, image stacks and single image files.

The detection stage requires the user to define an estimated radius of the cells, which can be problematic if cell sizes are different. Also, the performance of the cell-linkage phase can only be fully optimised by manually setting parameters such as the maximum linkage distance, but users may not be able to determine which values will generate the most accurate tracks. While the semi-automated design of TrackMate could be argued to be beneficial to allow fine-tuning, it could be considered less user-friendly than a fully automated method. Requiring manual input for each image is also problematic when analysing batch or high-throughput imaging data, as each TLM-movie may require different parameters.

CellProfiler is a popular bioimaging software proclaimed to be designed specifically for high-throughput image analysis while also possessing a user-friendly interface, containing multiple guided pipelines for quantifying cell features in images such as cell tracking in TLM-movies (McQuin et al, 2018). Unlike TrackMate, CellProfiler takes only image stacks and cannot analyse TLM-image files in video format directly, of which the conversion of the latter into the former into the former is time consuming and storage intensive. The cell detection algorithm involves binarization of the image and labelling of each cell, requiring input from the user to select the segmentation method. Like TrackMate, the LAP algorithm (Jaqaman et al, 2008) is used for cell-linkage and the parameters must be set by the user. This suggests CellProfiler may suffer from the same disadvantages in usability and analysing images in batches as TrackMate.

SpotTracker is a particle-based tracking plugin for Icy (de Chaumont et al, 2012), a bioimaging software similar to ImageJ/Fiji that offers the same versatility in analysing imaging files across different formats. The tracking algorithms requires more user input than TrackMate and CellProfiler, which uses a wavlet transform to detect spots only of user-defined sizes before the multiframe cell-linkage multiple hypothesis tracking (MHT) algorithm is used, as described by *Chenouard et al.* (2013). SpotTracker appears to be designed with user-control in mind, as it offers options allowing users to manually define which cells are to be tracked.

While the aforementioned software use algorithms that are designed to be versatile, the Tracking Challenges demonstrated no single cell tracking method can perform optimally across all types of imaging data (Chenouard et al, 2014; Ulman et al, 2017). The software also only generates tracks, usually as labelled cartesian coordinates, and do not provide methods for analysing them quantitatively, while supplemental software developed to analyse cell track data often focus on cell lineages, rather than their movement (Hilsenbeck et al, 2016). For these reasons, an approach designed specifically for tracking fluorescently labelled cells in whole-embryo fluorescent TLM-images of nonrodent amniotes could outperform present software while also having an incorporated algorithm to analyse the data, thus allowing for more a more quantitative analysis of CPC migration.

1.3 Cell Segmentation

Image segmentation is a form of image processing that refers to the separation of sets of pixels in an image into simplified homogenous regions, where OOIs of the foreground are distinguished from the background (Hamilton, 2009). Image segmentation is critical for detecting OOIs as well as characterising and extracting their features such as quantity, size, shape and positions, as in unprocessed images the intensities of both the foreground and background are not uniform and the object boundaries are undefined, meaning extracting said features directly would be challenging even in manual detection and implausible using algorithmic methods.

Segmentation algorithms designed for cell detection can be judged based on its power of capturing true cells (or true positives) and its tendency to capture false cells, also known as the false discovery rate (FDR). A perfect segmentation of an image with ideal quality would be sensitive enough to allow the identification of all true cells while also being specific to said cells with a FDR of zero, but this is rarely achievable due to limitations in current segmentation methods and imaging techniques, as cells may be lost in some frames or falsely detected due to low SNR, uneven lighting and overlapping of cells.

For cell tracking tools, it is essential that the segmentation method allows for a sensitive and specific detection of cells, as the proceeding cell-linkage algorithm cannot perform accurately when true cells are undetected or false cells are detected. The importance of segmentation is supported by the *Ulman et al.* review (2017), as for most of the CTC TLM-movies, the methods with the top cell-linkage performances also used the top performing segmentation algorithms.

In most current automated tracking methods, the segmentation algorithms used to capture cells follow a generalized principle shown in Figure 3, where the images are first pre-processed using filters, usually to remove noise that could falsely be captured as cells. The main segmentation processing step is used to detect the signals, but the algorithms can involve various combinations of approaches including using additional filters to detect particle-like “blobs” or edges (Wuttisarnwattana et al, 2014; Tinevez et al, 2017), binarizing the image into simplified regions (Lee et al, 1990; Ghaye et al, 2013), and transforming the image using morphological operations to ensure cells are presented as single objects (Malpica et al, 1997). The position of each cell is typically found by determining their features, such as centroids, or through detecting peak intesity maxima. Post-processing may also be used to filter non-cell signals based on features such as size or shape.

Cell segmentation using sophisticated machine learning techniques and convolutional neural networks can perform highly competitively compared to the more standard approaches, but their development is complex and requires a large amount of data to train (Sadanandan et al, 2017). This means that, despite their increasing in popularity, most current methods are developed with more basic principles.

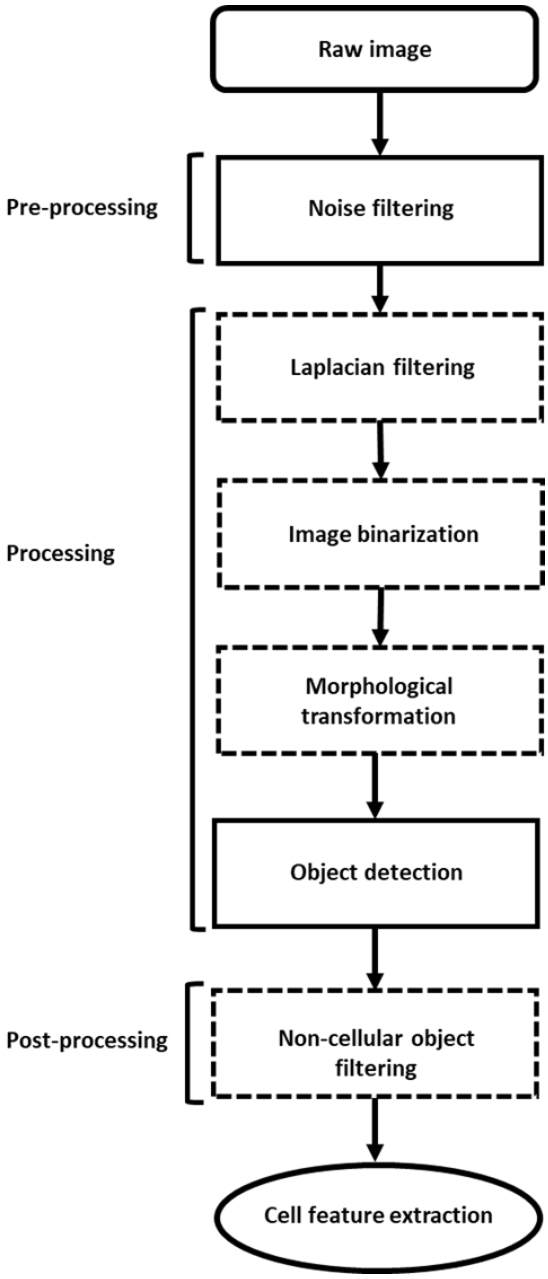

Figure 3. General approach for segmentation in cell tracking methods, involving pre-processing to remove noise, main processing where cells are detected and post-processing to further filter noise. Dotted boxes represent stages which are common, but not universal across all segmentation algorithms. Adapted from *Hamilton, 2009.*

Cell segmentation methods can vary greatly in sensitivity and specificity when capturing cells in different types of images, with algorithm reviews for both the CTC and PTC suggesting there is no single approach that performs optimally across all images produced using different microscopy techniques or within different biological contexts. In the case of FMIs with fluorescently labelled particle-like cells, features such as intense background noise defined by the signal-noise-ratio (SNR) and uneven lighting are common which can demand more complicated filtering or thresholding methods compared to DIC or PC images (Obara et al, 2013). The most widely used cell tracking software are applicable to many image types and biological contexts, usually involving semi-automated segmentations, which is likely why they are so versatile. A method designed specifically for detecting particle-like fluorescently labelled cells in TLM-images of whole embryos could potentially outperform current these software in said context however.

3.1 Image convolution

Convolving an image refers to a matrix operation that uses miniature matrices called kernels or convolution matrices, which can consist of different shapes, sizes and arrangements of values that act as weights. The kernel centers on each image pixel and determines the weighted sum of all local pixel intensities that fit within the kernel shape, which is then assigned said pixel (Elboher and Werman, 2012). The technique allows the filtering of specific pixel intensities from an image and can be used in cell segmentation approaches for removing noise, highlighting edges or detecting blobs.

(i) Noise filtering

The pre-processing stages of cell tracking algorithms usually involve noise removal, which is essential to prevent the detection of false cells, especially in FMIs, which often possess low SNRs compared to other imaging techniques. Image convolution is often used to smoothen or blur the images with the aim to reduce background regions with high intensity, which are assumed to be small points typically less than a few pixels in size.

Simple filters can use box blurs (figure 3A), where the kernel filter is designed with uniform values multiplied by a set fraction of one, but this method can lead to edges being too smooth to detect through the main segmentation process. In Gaussian blurring, shown in Figure 3B, the kernel values are produced by a Gaussian function, which can be used to filter noise while also retaining distinct edges (Babic and Mandic, 2003), making it preferable for cell detection. Some techniques can result in even more edge retention, such as median filtering (Niemisto et al, 2006).

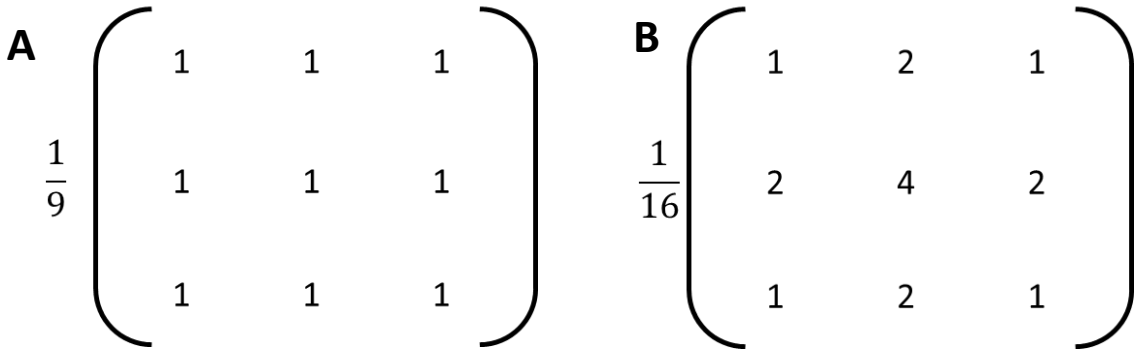

Figure 4. Kernels designed for noise filtering including a basic box filter (A) and a Gaussian filter (B).

(ii) Blob detection

For particle-like cells, image convolution can highlight them as small regions of high intensity against the background, after which they can be detected by thresholding and labelling, or by finding peak intensities across the image. For this purpose, Laplacian kernels are often used (Figure 5), which are distinguished by containing large values at the center and much smaller (often negative) values at the peripheral, or vice versa. Kernels can be automatically produced with such characteristics by applying a Laplacian operation on a Gaussian distribution, resulting in a Laplacian of Gaussian (LoG) filter, which is used in the TrackMate spot detector (Kong et al, 2013). A Difference of Gaussian (DoG) approach, where the difference of an image is found when applied with two Gaussian filters, can offer similar results to using LoG filters.

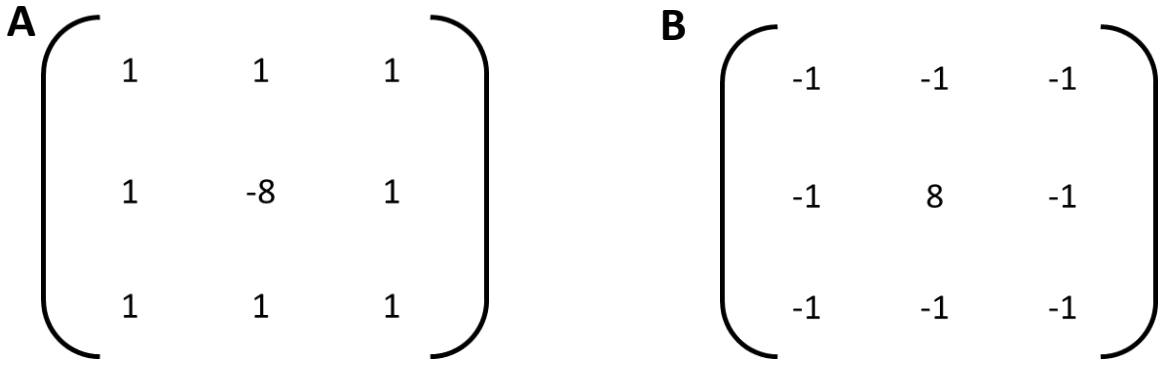

Figure 5. Laplacian kernels designed for blob detection for low intensity blobs (A) and high intesity blobs (B).

3.2 Thresholding

Thresholding is one of the most common segmentation techniques and involves categorizing pixels in an image into those with intensities that are above or below specified values, allowing the image to be partitioned into distinct regions (Hamilton, 2009). Typically, a single threshold value is used to binarize the image, which, assuming the intensities of the foreground are sufficiently distinct from those in the background, allows for OOIs such as cells to be separated from the background and detected.

In greyscale images where the pixel-intensity histogram displays two or more peaks a global thresholding approach, where the threshold value is the same for all pixels, is often used to detect cells. While the threshold value can be set manually, finding the value that allows for the greatest cell detection specificity and sensitivity can be time consuming, especially when analyzing a time-lapsed series of images, where the ideal threshold value may vary between frames. For this reason, automated methods are typically used to predict the ideal threshold value of an image based on the distribution of intensities. Techniques involving blob detection often use an automated or manual global threshold to homogenize the high intensity regions of cells following their convolution.

Otsu's thresholding was one of the earliest automated global techniques developed for greyscale image segmentation, ideally used when pixels display a bimodal distribution. Based on the assumption that the image foreground and background form each histogram peak as two separate classes, the algorithm finds the intensity with the maximum variance between classes and assigns it as the threshold value. Previous studies have successfully extracted cell features following the use of Otsu's thresholding in DIC/PC microscopy images or in FMIs with low background fluorescence (Obara et al, 2013; Du and Dua, 2010), as these images fit the assumptions of a bimodal distribution of pixel intensity. Microscopy images of fluorescently labelled cells are however often saturated with background noise that may lead to a pixel-intensity histogram that is unimodal, which is common in FMIs as a result of uneven lighting caused by background autofluorescence, overexpression of fluorescent proteins and photobleaching (Ghaye et al, 2013). In such images, Otsu's method and other global thresholding approaches are considered unsuitable as the background noise can be falsely detected as cells.

To resolve the segmentation issues found in images with unimodal pixel intensities, adaptive thresholding techniques (or dynamic thresholding) are often used, where a mutable threshold value is assigned to each pixel as opposed to all pixels in global techniques. Each adaptive threshold value is based on the intensities of local pixels, with the most common techniques including adaptive mean thresholding, where the threshold value is based on the mean of the local area, and adaptive Gaussian thresholding, where the value is based on a Gaussian weighted sum of the local pixel intensities.

There is however a tendency for FMIs to be over-segmented by local adaptive thresholding techniques, where the cells are often hollowed and fragmented into multiple spots, making it difficult to detect each cell. Morphological operations such as closing, where images are sequentially dilated and eroded to combine the disjointed fragments into whole cells, are often used in an attempt to correct this issue (Shen et al, 2018), but this itself could lead to issues where smaller cells could be conjoined to other cells or lost by the transformation, especially in images with particle-like cells. Thresholding is used by CellProfiler's CellTracker module, which may make it unsuitable for detecting fluorescent cells in noisy images.

3.3 Morphological operations

Mathematical morphology refers to operations which can transform binary images, the most basic operations of which include erosion and dilation. The operations work similarly to convolutional filtering, but instead applies a kernel with a specific shape called the structing element (Figure 6) across each pixel (Haralick et al, 1987). In erosion, if any pixels within the structuring element are not equal to 1, said pixel will be assigned 0, leading to portion of the object boundary being removed. In contrast, the dilation operation assigns 1 to the pixel if at least one other local pixel is also 1, causing the boundaries to expand. The size and shape a structuring element takes within a kernel has a significant impact on the result of the morphological operation, with those used on cells typically being elliptical due to their shape typically being circular.

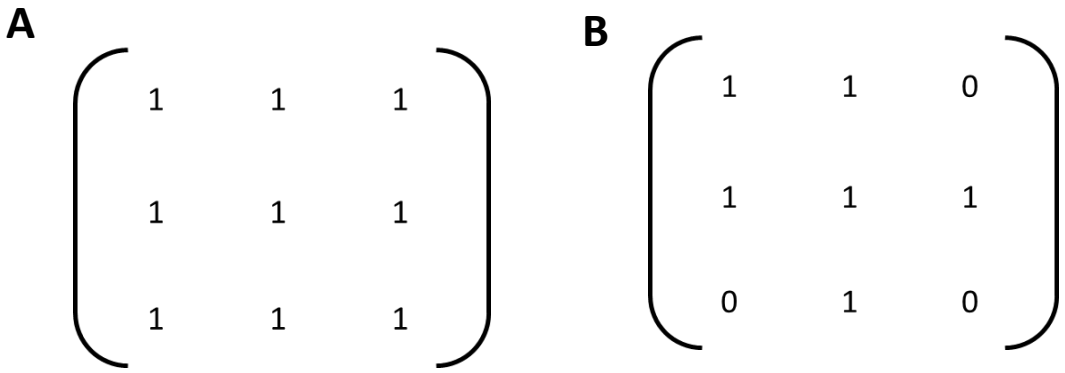

Figure 6. Kernels with structuring elements containing rectangles (A) and ellipses (B).

(i) Opening and closing

Opening and closing, which combine erosion and dilation operations by performing them consecutively, are common techniques used in the post-processing stages of cell detection following segmentation and binarization. Opening involves erosion followed by dilation, resulting in objects smaller than the structuring element being removed while mostly respecting the original size of larger objects which can be useful in determining cell boundaries (Di Rubeto et al, 2000). While opening has been used as a noise filter is some contexts (Argawai and Doermann, 2009), for filtering in cell images it could lead to a loss of lowly resolved particle-like cells. In contrast, closing involves image dilation followed by erosion, often leading to the joining of previously separate objects or the filling in of hollow objects. The technique has been used to de-hollow and reform single cells following their over-segmentation by adaptive thresholding (Shen et al, 2018), but it risks closely clustered cells becoming joined.

(ii) Watershed

Watershed transforms are commonly used in image segmentation to define boundaries of cells that overlap, which would make them indistinguishable in contour detection using binary thresholding alone, as well as labelling them (reviewed by Kornilov and Safonov, 2018). The algorithm is based on elements from topography, where the cells are considered points of low elevation with high elevation boundaries, after which cells are "flooded" as separate regions. Many watershed algorithms are based on an initial thresholded image that is distance transformed with markers located roughly at the centre of each cell being used as points of "flooding" (Salem et al, 2016), thus allowing the boundaries of cells to be distinguished.

3.4 Feature extraction

Detection association-based cell tracking algorithms require features of cells to be detected across frames, with the most universal being position but can also include intensity, size and spatial features, as reviewed by *Meijering et al.* (2012). For tracking particle-like cells of near uniform size, the position and intensity are often the only features used, since it is impossible to distinguish other features. Detection usually involves finding a centroid to each cell, which can occur following Laplacian filtering, thresholding, watershed transforming, or a combination of the three.

(i) Contour detection

A common method of extracting cell centroid positions in binarized images involves first tracing the boundaries of an object using contours, where an active model is fitted across a boundary based the energinicity of the edge and the surrounding regions (Kass et al, 1988). The method offers a robust approach to cell detection which makes no prior assumptions about the cell sizes and allows the extraction of multiple cell features including centroid position, intensity, size and shape (Molnar et al, 2016). A disadvantage is that the method could become computationally costly as cell populations increase.

(ii) Extrema detection

Extrema detection is an alternate method of detecting cells which is most effective following segmentation processes that involve Laplacian filtering or other blob detection approaches and is commonly incorporated in particle-tracking tools such as TrackMate (Kong et al, 2013). Particle-like cells can be detected by applying a DoG segmenter, from which sharp local maximas of intensity are detected before each pixel around each maxima are compared to local neighbours within a defined area, where the highest intensities are determined as the centre of the cell (Lowe, 2004). The method is computationally efficient compared to contour detection, but current algorithms suffer from requiring an assumed value for cell diameter to compute which points of extrema can be detected as cells. This means a cell too close to another could be excluded, or a larger cell could be detected as two.

1.4 Cell linkage

Tracking cells in TLM-images involves linking the captured cells across frames, with automated tracking of multiple cells requiring solutions to numerous problems that can prevent the generation of accurate and complete tracks. Algorithms are generally based on a linkage-decision that must determine which cells are to be linked between frames across TLM-movies with large numbers of that sometimes move sporadically. A cell may also be detected in some image frames, but missing in others, meaning the algorithm must interpolate across a gap to produce a complete track, referred to as gap-closing. Often movies involve cells that cluster closely together or overlap, so the method must also be able to handle instances where cells converge, diverge and cross-over each other's tracks.

Many different algorithms involving various approaching to solving these problems have been designed for automatically tracking cells in TLM-images. As shown in the Tracking Challenge reviews of cell tracking methods, the performance of specific algorithms in generating accurate and complete tracks can vary depending on the imaging techniques used to produce the images and factors such as the presence of fluorescent labels, image resolution, the SNR and the frame capture rate.

The suitability of a tracking algorithm may also depend on features of the cells such as their size, shape, motile activity, mitotic potential, uniformity and the distinguishability of intracellular structures, but as previously mentioned, contrast to movies in the Cell Tracking Challenge, some TLM-movies involve cells that have no visible intracellular features, do not divide and appear as fluorescent particle-like "spots". Analysing such cells could involve approaches from particle tracking, which despite being designed for fluorescent intracellular structures, attempt to solve issues regarding gap closing and overlapping events rather than lineage tracing. The tracking algorithms presented in a review of solutions to the Particle Tracking Challenge by *Chenouard et al.* (2014) showed similarities to approaches used to solve the Cell Tracking Challenge and many of them are featured in popular "cell tracking" tools such as TrackMate, CellProfiler: CellTracker and SpotTracker.

As previously mentioned, an algorithm's power in generating accurate tracks depends heavily the specificity and sensitivity of the cell detection during the preceding segmentation stage, as the tracking methods are designed with the assumption that individual cells can be continuously detected across multiple image frames. This is possibly supported by the *Ulman et al.* review, as for most of the Cell Tracking Challenge TLM-movies, the method with the top tracking performance included the top performing segmentation algorithm.

Tracking algorithms generally follow different principles, with some, such as the LAP algorithm in TrackMate and CellProfiler: CellTracker following a frame-to-frame decision when linking cells, followed by a filling in of gaps (Jaqaman et al, 2008). The MHT algorithm in SpotTracker however follows a multiframe approach, where tracks are built across frames by finding the best fit between past and future frames (Chenouard et al, 2013). Most methods are based on the Nearest Neighbour algorithm, which is usually used to identify cells in consecutive frames that are distally close, but it can also find cells that are similar based on intensity, size or shape.

Chapter 2. Project design and aims

The objectives of this project are to assess the performance of existing cell tracking software in capturing the migration of GFP-labelled CPCs in fluorescent TLM-movies of the early chick embryo and to identify potential shortcomings in cell detection and linkage across the image-series. We then aim to improve these flaws by testing a variety of computer vision and machine learning techniques, from which we will select the highest performing approaches for our specific TLM-movies, which will then be used to quantitively characterise differences in CPC migration patterns in chick embryos with varying gain- or loss-of-function interventions. Finally, we will build our algorithms into a user-friendly software tool designed to meet many of the usability criteria defined by *Carpenter et al.* (2012) for bioimaging software.

All TLM-movies used in this project were provided by the Munsterberg group, members of which also contributed to their generation as well as the culturing and labelling of chick embryos, described in Chapter 3.1 and 3.2 respectively. The limitations of existing cell tracking software and the need for tools designed specifically for tracking fluorescent cells across TLM-images of whole embryos was first noted by the group, which coincides with the conclusions by *Chenouard et al.* (2014) and *Ulman et al.* (2017) that no single tracking algorithm has been shown to perform optimally across all imaging data and biological contexts.

Python 3.7 was chosen to design the tool due to it being a widely used programing language for computer vision and data analysis while possessing an intuitive syntax for more idiomatic code. It also supported by many powerful libraries such as OpenCV for general computer vision techniques, Numpy for array and matrix operations, and Scikit-learn for machine learning algorithms, which are all compiled modules that can perform efficiently. OpenCV offers basic functions for image processing, including blurring for noise filtering, global and adaptive techniques for thresholding, and morphological operations for watersheds. Scikit-learn functions could be useful in the cell-linkage algorithm, offering basic tools such as K-Nearest Neighbor to find close cells in different frames, different types of regression models to interpolate and extrapolate cell trajectories and advanced techniques like decision trees to determine which cells should be linked.

Chapter 3. Methodology

3.1 Embryo culturing and GFP-labelling

Fertile brown chicken eggs were grown in a humidified incubator at 38^{o}C until reaching HH3, following which the embryos were harvested and cultured as described by *Chapman et al.* (2001). The mid-anterior primitive streak where CPCs are localised was microinjected with IRES-GFP expression plasmids following protocols described by *Yue et al.* (2008). Expression plasmids were transfected into CPCs through electroporation using methods described by *Yang et al.* (2002), following which embryos were left to heal overnight.

3.2 Time-lapsed-microscopy of embryos

GFP-labelled embryos were cultured in six-well plates, after which long-term time-lapsed-image-series were generated using an inverted wide-field microscope (Axiovert, Ziess), with brightfield and fluorescent images being captured at 5 minute time-points across 24 hours. Time-lapses from HH3-4 up to HH8-10 were exported as ZVI files containing images that were exclusively greyscale.

3.3 Cell capturing with software tools

Raw ZVI TLM-movies were imported into ImageJ with the Fiji plugins, following which the brightfield and fluorescent channels were separated, the former being discarded. A ground-truth value for cell counts in each image was found through manual counting using ImageJ at three separate points, including the first, mid and ¾ frame, which was chosen instead of the final frame because fluorescent signals tend to dissipate at the end of TLM-movies. We then tested the cell tracking tools TrackMate, CellProfiler: Cell tracker, SpotTracker and NucliTrack.

TrackMate was initiated with median filtering and a blob diameter set to 5. LoG and DoG spot detectors were used consecutively for comparison. Particle-linking was run with standard settings, as this is not relevant for this instance, following which the track data was exported and the cell count for each frame was extracted. We did not use CellProfiler, because the thresholding step was slow performing (>60min) and SpotTracker failed to detect many cells (<5). We also tested NucliTrack, but the programme consistently crashed in the segmentation stage.

3.4 Image formatting and pre-processing

Raw TLM-images in ZVI format were converted to AVI video format using Bioformats in ImageJ, after which the brightfield channel was separated from the fluorescent green channel. In Python 3.7, OpenCV and Numpy were used to convert the image matrices into arrays, following which noise filtering was performed using a median blur function, which has previously been shown to successfully retain edges of objects (Niemisto et al, 2006).

3.5 Laplacian filtering and thresholding of images

Multiple Laplacian kernels with different positive central values and of differing sizes were generated using Numpy, each of which were used to convolve the noise filtered image-series using a 2D filter function. The kernel with the least noise but highest cell retention was subsequently binarized through Otsu thresholding. For comparison, images without the Laplacian were also thresholded using an Otsu and Gaussian adaptive function.

3.6 Watershed transformation of images

A marker-based Watershed was applied using morphological operations and the Watershed function in OpenCV. A distance transform was applied to the binarized image-series followed by a threshold to establish small markers near the centre of each cell. The assumed background boundary was defined by dilating the image and subtracting the markers. Markers were labelled before applying the Watershed function on the original binary image. Cells were segmented by applying a black outer boundary.

3.7 Contour and centroid detection

Contours of cell boundaries were found using an OpenCV function, of which the cartesian coordinates for their centroids were determined using an image moments function. The centroid positions for each image-frame were structured into Numpy arrays before being counted. Centroids from each array were recursively drawn onto frames to produce a basic trajectory visualization.

Chapter 4. Current Progress

4.1 Software cell detection

A TLM-movie produced using FMI of an early chick embryo with GFP-labelled CPCs, of which no additional treatments were applied, was selected as training data for the segmentation algorithm. The time-lapse (Figure 7), contained 206 image-frames and showed abnormal migration of CPCs, with most moving laterally rather than anteriorly, making it difficult to determine the final HH stage, but it starts at HH4 with CPCs already having left the primitive streak. The fluorescent channel in AVI format was open by Fiji, after which the ground-truth number of cells were counted manually for image-frames 1, 103 and 155 using Fiji/ImageJ.

We then tested the ImageJ plugin TrackMate for cell detection, finding both LoG and DoG spot tracking methods performed optimally when initiated with median filtering and a blob diameter set to 5. Particle-linking was run with standard settings, as this is not relevant for this instance, following which the track data was exported and the cell count for each frame was extracted. Despite consistent testing, SpotTracker continuously failed to capture a representative sample of cells (>10), while CellProfiler: CellTracker had a long runtime (>60 mins) that made optimisation inefficient and in every NucliTrack test, the programme crashed during segmentation. For this reason, these software were excluded from the comparison.

4.2 Cell segmentation

Our custom algorithm used a median filter to remove small regions of background noise whilst retaining the spatial integrity of the cells. As shown in Figure 7, smaller points of background noise were removed from the image, while the structure of larger regions of fluorescence were still distinguishable.

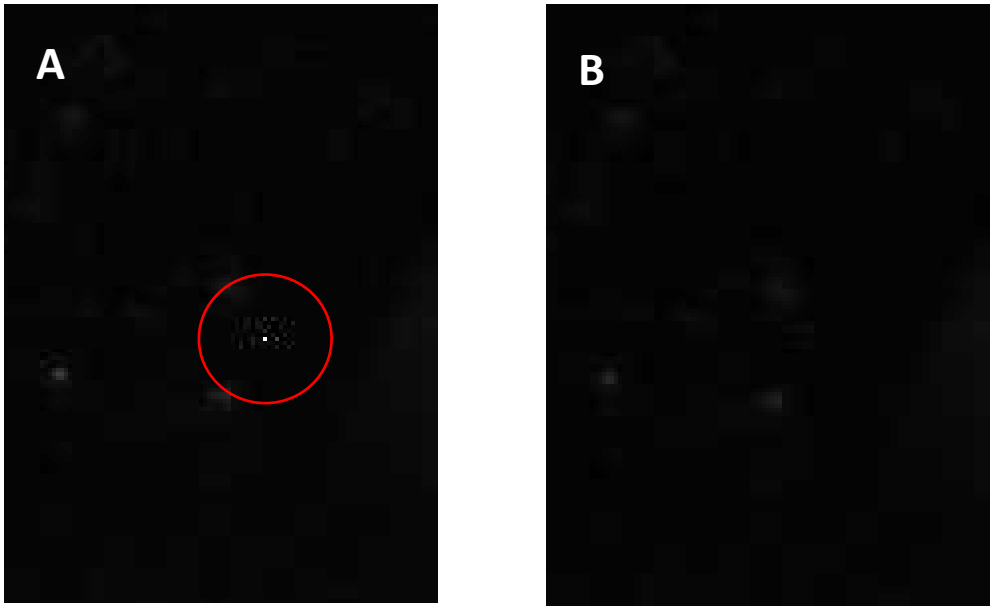

Figure 7. Image partition of GFP-labelled TLM-movie of chick embryo training data. The raw image shows a noisy artefact shown in red (A), which is subsequently removed by median filtering (B). Large fluorescent regions are still distinguishable.

We tested the use of Laplacian filtering on the denoised image-series to identify the optimal Laplacian kernel size and structure. Kernels of sizes 9x9 were generated with central values 30, 60 and 90, shown in Figure 8, where we found a central intensity of 60 performed most optimally.

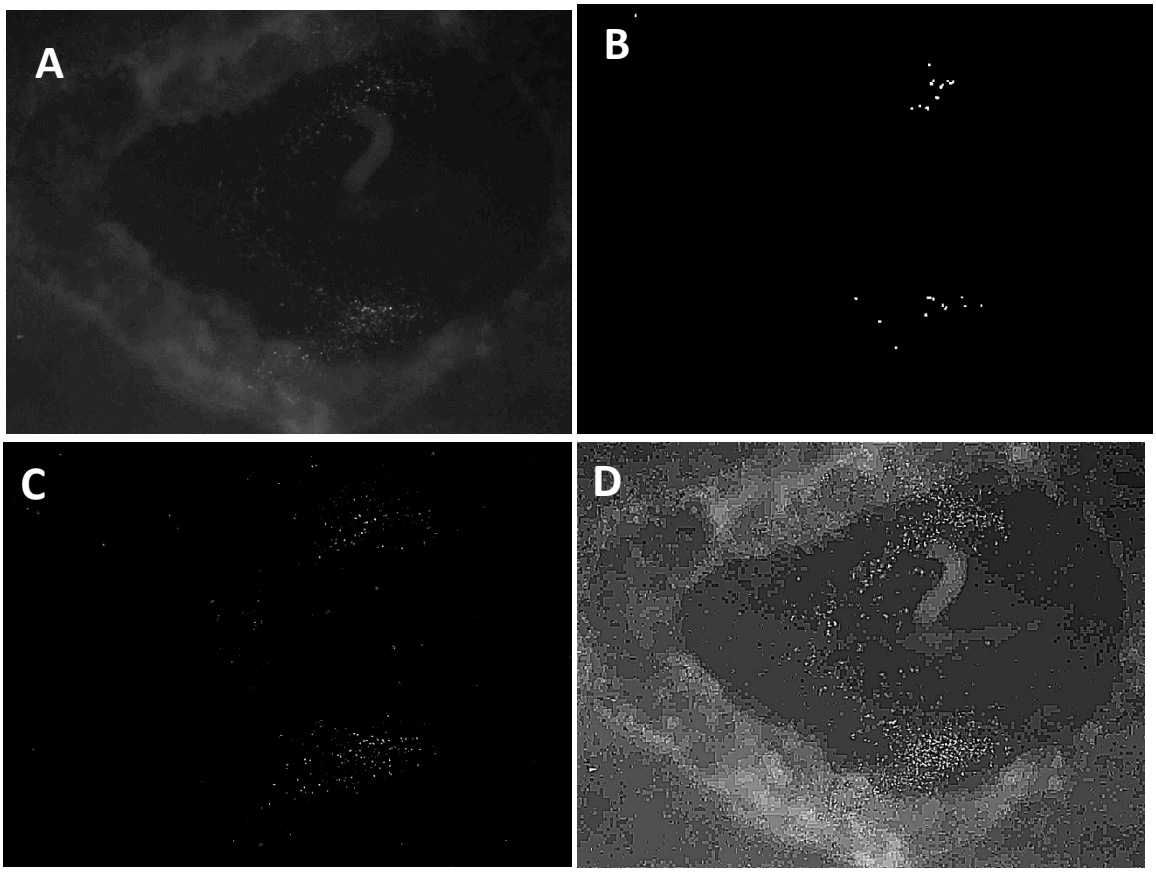

Figure 8. Images from training TLM-movie data without Laplacian filtering (A) or filtering using a 9x9 Laplacian kernel with a central value of 30 (B – with dilation), 60 (C) and 90 (D).

To binarize the image, we applied an Otsu threshold on the Laplacian filtered image, as well as both an Otsu and adaptive Gaussian threshold on a denoised image for comparison as shown in Figure 9. Otsu thresholding resulted in under-segmentation, with large regions of fluorescent background being classed the same as cells, with those that enter these regions being undistinguishable. The Adaptive Gaussian approach over-segmented the images, with cells appearing as hollow and broken clusters. The Laplacian filter more optimally distinguishes cells as fluorescent blobs that are separate from regions of background fluorescence.

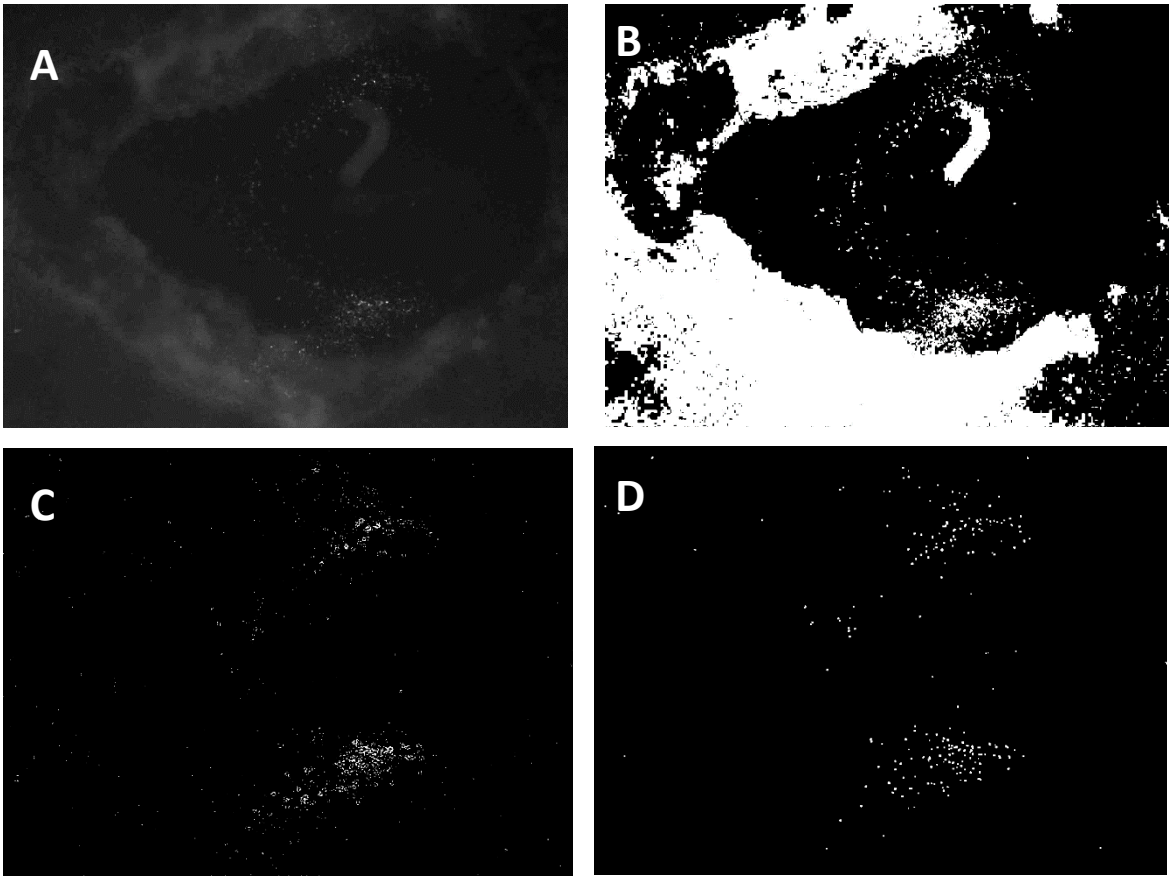

Figure 9. Images from training TLM-movie data including images that were pre-segmented (A), globally thresholded by Otsu's method (B), thresholded by an adaptive Gaussian (C) or filtered by a Laplacian kernel (D).

The marker-based watershed transform was applied to binarized Laplacian filtered image (Figure 10), which successfully distinguished the boundaries of cells for the extraction of their features. The centroid was extracted for each cell, which were used to create a trajectory visualization across the time-lapse (Figure 11).

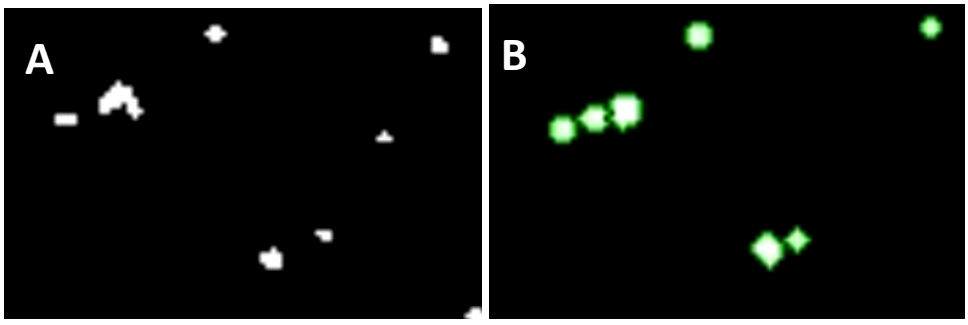

Figure 10. Partition of images from training TLM-movie data with Laplacian filtered and binarized cells. Includes raw images (A) and images following the Watershed transform (B).

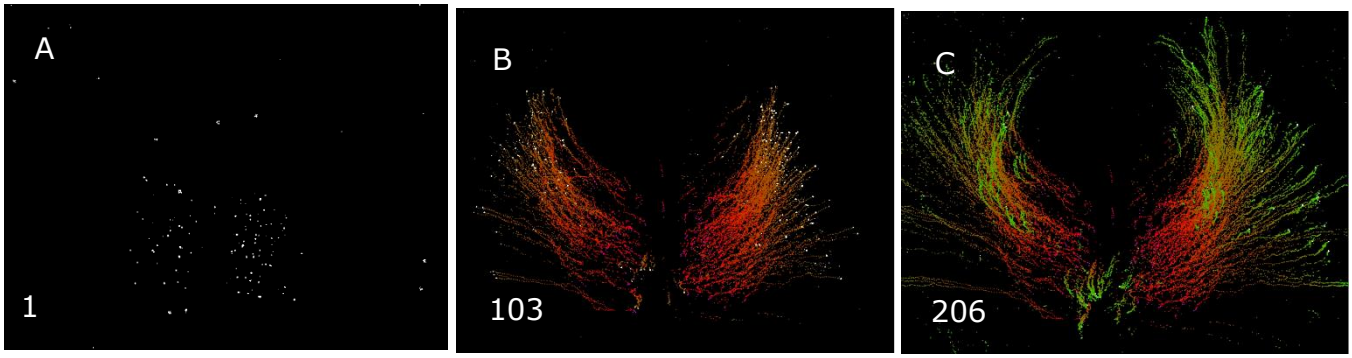

Figure 11. Migration trajectories of GFP-labelled CPCs in an untreated early chick embryo starting at HH4. At frame 1 (A), cells have left the mid-anterior primitive streak, after which frame 103 (B) shows a bilateral migration, with some cells moving to the anterior of the embryo and others move laterally. Frame 206 (C) shows only a few cells migrated to the medial-anterior of the embryo.

4.2 Comparison of methods

We found the average cell count, as shown in Figure 12, was 361.7 (SD 115.1) for the ground-truth, 373.3 (SD 138.2) for our convolution-watershed method, 523.3 (SD 212.9) using TrackMate with LoG settings and 320.0 (SD 146.7) in the DoG detector. Compared to ground-truth cell count, our detection method showed the smallest difference at 11.6, while in TrackMate, the LoG method showed at least 161.6 false positives and DoG had 41.7 false negative detections. Differences between detection methods were not significant ($P > 0.05$).

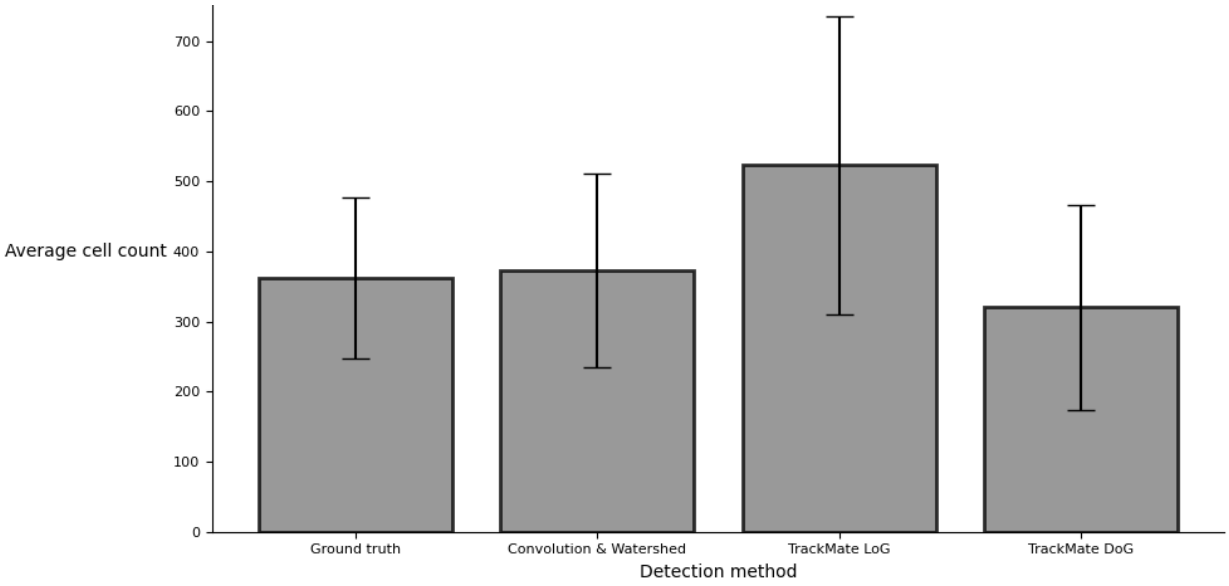

Figure 12. Different cell detection methods in comparison to a manually counted ground-truth, including our custom convolution and watershed algorithm, and the TrackMate detectors using Laplacian of Gaussian (LoG) and Difference of Gaussian (DoG).

Chapter 5. Future goals

5.1 Automated segmentation

Currently, the segmentation algorithm uses a Laplacian filter optimised for this specific TLM-movie, but in other movies, a different size or structure of the Laplacian kernel could outperform our current one. We will investigate automated segmentation approaches through dynamic Laplacian filters, where multiple kernel shapes and sizes are automatically used to filter an image to find the most appropriate.

5.2 Cell tracking algorithm

The cell tracking algorithm will be designed firstly by assessing the tracking methods used by present software and shown in the CTC and PTC reviews. A simple method will firstly be designed to link cells frame-to-frame using a Nearest Neighbour algorithm, which is expected to result in false linkages and gaps in the tracks. This will be improved by using regression tools in Python with the Scikit-learn libary to extrapolate the trajectories of cells and predict their expected position in other frames, which with the angle of a cells trajectory between frames may be incorporated into a decision as to which cells should be linked. Gap closing could be prevented by using regression modelling to interpolate between multiple frames, thus linking the tracks. As cell tracking algorithms are complex and can sometimes require extensive mathematical experience to develop, if our custom algorithm fails to perform as successfully as current algorithms, these will be adapted into our method and the most competitive approach will be selected for cell tracking.

5.3 Quantification of CPC migration

After generating complete tracks, an algorithm will be designed to quantify cell behaviours across each TLM-movie, which could involve the use of different classification techniques in the Scikit-lean library due to the large number of cells. Cells will be classified based on their exit angle, overall migratory distance and their tendency to cluster near other cells. The different TLM-movies will be compared to others with different gain- or loss-of-function interventions to determine if there are significant differences between CPC migratory behaviours.

5.4 Software development

The collection of algorithms will be packaged into a software, which will be developed using the Tkinter Python library. The software will be designed to be user-friendly with the potential to analyse batches of imaging data and will have automated settings that can be optimised by the user. To meet the criteria set by *Carpenter et al.* (2012), it will be able to output detection or track results in a format that can be used by other analysis tools, or alternatively be able to use track data from other software for quantification.

5.5 Gantt chart

Task	Oct	Nov	Dec	Jan	Feb	Mar	Apr	May	Jun	Jul	Aug		Sept
Review current software													
Develop segmentation methods													
Compare segmentation methods													
Develop cell linkage method													
Develop cell classification method													
Compare TLM movies with different interventions													
Automate segmentation method													
Incorporate algorithms into software													
Write thesis													

Acknowledgements

We would like to thank the following members of the Munsterberg group for handling embryos and generating the TLM-movies: Melissa Antoniou-Kourounioti, Timothy Wood and Sophie Stephenson.

References:

Agrawal M, Doermann D (2009) Clutter Noise Removal in Binary Document Images. 2009 10th International Conference on Document Analysis and Recognition. 556–560.

Babic ZV, Mandic DP (2003) An efficient noise removal and edge preserving convolution filter. 6th International Conference on Telecommunications in Modern Satellite, Cable and Broadcasting Service, 2003. 538–541.

Carpenter AE, Kamentsky L, Eliceiri KW (2012) A call for bioimaging software usability. Nature Methods 9:666–670.

Chapman SC, Collignon J, Schoenwolf GC, Lumsden A (2001) Improved method for chick whole-embryo culture using a filter paper carrier. Dev Dyn 220:284–289.

Chenouard N, Bloch I, Olivo-Marin J-C (2013) Multiple Hypothesis Tracking for Cluttered Biological Image Sequences. IEEE Transactions on Pattern Analysis and Machine Intelligence 35:2736–3750.

Chenouard N, Smal I, de Chaumont F, Maška M, Sbalzarini IF, Gong Y, Cardinale J, Carthel C, Coraluppi S, Winter M, Cohen AR, Godinez WJ, Rohr K, Kalaidzidis Y, Liang L, Duncan J, Shen H, Xu Y, Magnusson KEG, Jaldén J, Blau HM, Paul-Gilloteaux P, Roudot P, Kervrann C, Waharte F, Tinevez J-Y, Shorte SL, Willemse J, Celler K, van Wezel GP, Dan H-W, Tsai Y-S, de Solórzano CO, Olivo-Marin J-C, Meijering E (2014) Objective comparison of particle tracking methods. Nat Methods 11:281–289.

Chuai M, Hughes D, Weijer CJ (2012) Collective Epithelial and Mesenchymal Cell Migration During Gastrulation. Curr Genomics 13:267–277.

Colas J-F, Lawson A, Schoenwolf GC (2000) Evidence that translation of smooth muscle alpha-actin mRNA is delayed in the chick promyocardium until fusion of the bilateral heart-forming regions. Developmental Dynamics 218:316–330.

Cooper S, Barr AR, Glen R, Bakal C (2017) NucliTrack: an integrated nuclei tracking application. Bioinformatics 33:3320–3322.

de Chaumont F, Dallongeville S, Chenouard N, Hervé N, Pop S, Provoost T, Meas-Yedid V, Pankajakshan P, Lecomte T, Le Montagner Y, Lagache T, Dufour A, Olivo-Marin J-C (2012) Icy: an open bioimage informatics platform for extended reproducible research. Nature Methods 9:690–696.

DeHaan RL (1963) Migration patterns of the precardiac mesoderm in the early chick embryo. Experimental Cell Research 29:544–560.

Di Rubeto C, Dempster A, Khan S, Jarra B (2000) Segmentation of blood images using morphological operators. Proceedings 15th International Conference on Pattern Recognition. ICPR-2000. 397–400.

Dormann D, Weijer CJ (2006) Imaging of cell migration. EMBO J 25:3480–3493.

Du X, Dua S (2010) Segmentation of Fluorescence Microscopy Cell Images Using Unsupervised Mining. Open Med Inform J 4:41–49.

Elboher E, Werman M (2012) Efficient and accurate Gaussian image filtering using running sums. 2012 12th International Conference on Intelligent Systems Design and Applications (ISDA). 897–902.

Fan H, Sakamoto N, Aoyama H (2018) From the primitive streak to the somitic mesoderm: labeling the early stages of chick embryos using EGFP transfection. Anat Sci Int 93:414–421.

Ghaye J, Kamat MA, Corbino-Giunta L, Silacci P, Vergères G, Micheli GD, Carrara S (2013) Image thresholding techniques for localization of sub-resolution fluorescent biomarkers. Cytometry Part A 83:1001–1016.

Gittenberger-de Groot AC, Bartelings MM, Deruiter MC, Poelmann RE (2005) Basics of Cardiac Development for the Understanding of Congenital Heart Malformations. Pediatric Research 57:169–176.

Gräper L (1929) Die Primitiventwicklung des Hühnchens nach stereokinematographischen Untersuchungen, kontrolliert durch vitale Farbmarkierung und verglichen mit der Entwicklung anderer Wirbeltiere. W Roux' Archiv f Entwicklungsmechanik 116:382–429.

Hamburger V, Hamilton HL (1951) A series of normal stages in the development of the chick embryo. J Morphol 88:49–92.

Hamilton N (2009) Quantification and its Applications in Fluorescent Microscopy Imaging. Traffic 10:951–961.

Haralick RM, Sternberg SR, Zhuang X (1987) Image Analysis Using Mathematical Morphology. IEEE Transactions on Pattern Analysis and Machine Intelligence PAMI-9:532–550.

Hatada Y, Stern CD (1994) A fate map of the epiblast of the early chick embryo. Development 120:2879–2889.

Hilsenbeck O, Schwarzfischer M, Skylaki S, Schauberger B, Hoppe PS, Loeffler D, Kokkaliaris KD, Hastreiter S, Skylaki E, Filipczyk A, Strasser M, Buggenthin F, Feigelman JS, Krumsiek J, van den Berg AJJ, Endele M, Etzrodt M, Marr C, Theis FJ, Schroeder T (2016) Software tools for single-cell tracking and quantification of cellular and molecular properties. Nature Biotechnology 34:703–706.

Imaris for Tracking - Imaris. In: Oxford Instruments. https://imaris.oxinst.com/products/imaris-for-tracking. Accessed 14 Apr 2020

Jaqaman K, Loerke D, Mettlen M, Kuwata H, Grinstein S, Schmid SL, Danuser G (2008) Robust single-particle tracking in live-cell time-lapse sequences. Nature Methods 5:695–702.

Kass M, Witkin A, Terzopoulos D (1988) Snakes: Active contour models. Int J Comput Vision 1:321–331.

Kong H, Akakin HC, Sarma SE (2013) A Generalized Laplacian of Gaussian Filter for Blob Detection and Its Applications. IEEE Transactions on Cybernetics 43:1719–1733.

Kornilov AS, Safonov IV (2018) An Overview of Watershed Algorithm Implementations in Open Source Libraries. Journal of Imaging 4:123.

Ladd AN, Yatskievych TA, Antin PB (1998) Regulation of avian cardiac myogenesis by activin/TGFbeta and bone morphogenetic proteins. Dev Biol 204:407–419.

Le T, Chong J (2016) Cardiac progenitor cells for heart repair. Cell Death Discov 2:16052.

Lowe DG (2004) Distinctive Image Features from Scale-Invariant Keypoints. International Journal of Computer Vision 60:91–110.

Malpica N, de Solórzano CO, Vaquero JJ, Santos A, Vallcorba I, García-Sagredo JM, del Pozo F (1997) Applying watershed algorithms to the segmentation of clustered nuclei. Cytometry 28:289–297.

Martinsen BJ (2005) Reference guide to the stages of chick heart embryology. Developmental Dynamics 233:1217–1237.

Marvin MJ, Di Rocco G, Gardiner A, Bush SM, Lassar AB (2001) Inhibition of Wnt activity induces heart formation from posterior mesoderm. Genes Dev 15:316–327.

McColl J, Mok GF, Lippert AH, Ponjavic A, Muresan L, Münsterberg A (2018) 4D imaging reveals stage dependent random and directed cell motion during somite morphogenesis. Sci Rep 8:12644.

McQuin C, Goodman A, Chernyshev V, Kamentsky L, Cimini BA, Karhohs KW, Doan M, Ding L, Rafelski SM, Thirstrup D, Wiegraebe W, Singh S, Becker T, Caicedo JC, Carpenter AE (2018) CellProfiler 3.0: Next-generation image processing for biology. PLoS Biol 16.

Meijering E, Dzyubachyk O, Smal I (2012) Chapter nine - Methods for Cell and Particle Tracking. Methods in Enzymology. 504:183–200.

Molnar C, Jermyn I, Kato Z, Rahkama V, Ostling P, Mikkonen P, Pietiäinen V, Horvath P (2016) Accurate Morphology Preserving Segmentation of Overlapping Cells based on Active Contours. Scientific Reports 6:32412.

Myers CT, Krieg PA (2013) BMP-mediated specification of the erythroid lineage suppresses endothelial development in blood island precursors. Blood 122:3929–3939.

Niemisto A, Selinummi J, Saleem R, Shmulevich I, Aitchison J, Yli-Harja O (2006) Extraction of the Number of Peroxisomes in Yeast Cells by Automated Image Analysis. 2006 International Conference of the IEEE Engineering in Medicine and Biology Society. 2353–2356.

Obara B, Roberts MA, Armitage JP, Grau V (2013) Bacterial cell identification in differential interference contrast microscopy images. BMC Bioinformatics 14:134.

Obara B, Roberts MA, Armitage JP, Grau V (2013) Bacterial cell identification in differential interference contrast microscopy images. BMC Bioinformatics 14:134.

Osei-Sarfo K, Gudas LJ (2014) Retinoic acid suppresses the canonical Wnt signaling pathway in embryonic stem cells and activates the noncanonical Wnt signaling pathway. Stem Cells 32:2061–2071.

Osmond MK, Butler AJ, Voon FC, Bellairs R (1991) The effects of retinoic acid on heart formation in the early chick embryo. Development 113:1405–1417.

Pinto-Teixeira F, Muzzopappa M, Swoger J, Mineo A, Sharpe J, Lopez-Schier H (2013) Intravital imaging of hair-cell development and regeneration in the zebrafish. Front Neuroanat 7.

Sadanandan SK, Ranefall P, Le Guyader S, Wählby C (2017) Automated Training of Deep Convolutional Neural Networks for Cell Segmentation. Scientific Reports 7:1–7.

Salem N, Sobhy NM, Dosoky ME (2016) A Comparative Study of White Blood cells Segmentation using Otsu Threshold and Watershed Transformation. 1 3:15–15.

Schoenwolf GC, Garcia-Martinez V (1995) Primitive-streak origin and state of commitment of cells of the cardiovascular system in avian and mammalian embryos. Cell Mol Biol Res 41:233–240.

Schultheiss TM, Burch JB, Lassar AB (1997) A role for bone morphogenetic proteins in the induction of cardiac myogenesis. Genes Dev 11:451–462.

Shen SP, Tseng H, Hansen KR, Wu R, Gritton HJ, Si J, Han X (2018) Automatic Cell Segmentation by Adaptive Thresholding (ACSAT) for Large-Scale Calcium Imaging Datasets. eNeuro 5.

Song J, McColl J, Camp E, Kennerley N, Mok GF, McCormick D, Grocott T, Wheeler GN, Münsterberg AE (2014) Smad1 transcription factor integrates BMP2 and Wnt3a signals in migrating cardiac progenitor cells. PNAS 111:7337–7342.

Stalsberg H, DeHaan RL (1969) The precardiac areas and formation of the tubular heart in the chick embryo. Developmental Biology 19:128–159.

Tanenbaum ME, Gilbert LA, Qi LS, Weissman JS, Vale RD (2014) A Protein-Tagging System for Signal Amplification in Gene Expression and Fluorescence Imaging. Cell 159:635–646.

Ulman V, Maška M, Magnusson KEG, Ronneberger O, Haubold C, Harder N, Matula P, Matula P, Svoboda D, Radojevic M, Smal I, Rohr K, Jaldén J, Blau HM, Dzyubachyk O, Lelieveldt B, Xiao P, Li Y, Cho S-Y, Dufour AC, Olivo-Marin J-C, Reyes-Aldasoro CC, Solis-Lemus JA, Bensch R, Brox T, Stegmaier J, Mikut R, Wolf S, Hamprecht FredA, Esteves T, Quelhas P, Demirel Ö, Malmström L, Jug F, Tomancak P, Meijering E, Muñoz-Barrutia A, Kozubek M, Ortiz-de-Solorzano C (2017) An Objective Comparison of Cell Tracking Algorithms. Nat Methods 14:1141–1152.

Volocity Software. In: Quorum Technologies. http://quorumtechnologies.com/index.php/component/content/category/31-volocity-software. Accessed 14 Apr 2020

Voronov DA, Alford PW, Xu G, Taber LA (2004) The role of mechanical forces in dextral rotation during cardiac looping in the chick embryo. Developmental Biology 272:339–350.

Waddington CH (1933) Induction by the endoderm in birds. W Roux' Archiv f Entwicklungsmechanik 128:502–521.

Wetzel R (1929) Untersuchungen am Huhnchen. Die Entwicklung des Keims wahrend der erste beiden Bruttage. Archiv f Entwicklungmechanik 119:188–321.

Wuttisarnwattana P, Gargesha M, Hof W van't, Cooke KR, Wilson DL (2016) Automatic Stem Cell Detection in Microscopic Whole Mouse Cryo-imaging. IEEE Trans Med Imaging 35:819–829.

Yang X, Dormann D, Münsterberg AE, Weijer CJ (2002) Cell Movement Patterns during Gastrulation in the Chick Are Controlled by Positive and Negative Chemotaxis Mediated by FGF4 and FGF8. Developmental Cell 3:425–437.

Yatskievych TA, Ladd AN, Antin PB (1997) Induction of cardiac myogenesis in avian pregastrula epiblast: the role of the hypoblast and activin. Development 124:2561–2570.

Yue Q, Wagstaff L, Yang X, Weijer C, Münsterberg A (2008) Wnt3a-mediated chemorepulsion controls movement patterns of cardiac progenitors and requires RhoA function. Development 135:1029–1037.

Zhang XY, Rodaway ARF (2007) SCL-GFP transgenic zebrafish: In vivo imaging of blood and endothelial development and identification of the initial site of definitive hematopoiesis. Developmental Biology 307:179–194.